Secretory Protein Decondensation as a Distinct, Ca^{2+}-mediated Event during the Final Steps of Exocytosis in *Paramecium* Cells

M. BILINSKI, H. PLATTNER, and H. MATT
Faculty of Biology, University of Konstanz, Konstanz, Federal Republic of Germany

ABSTRACT The contents of secretory vesicles ("trichocysts") were isolated in the condensed state from *Paramecium* cells. It is well known that the majority portion of trichocysts perform a rapid decondensation process during exocytosis, which is visible in the light microscope. We have analyzed this condensed→decondensed transition in vitro and determined some relevant parameters. In the condensed state, free phosphate (and possibly magnesium) ions screen local surplus charges. This is supported by x-ray spectra recorded from individual trichocysts (prepared by physical methods) in a scanning transmission electron microscope. Calcium, as well as other ions that eliminate phosphate by precipitation, produces decondensation in vitro. Under in vivo conditions, Ca^{2+} enters the vesicle lumen from the outside medium, once an exocytic opening has been formed. Consequently, within the intact cell, membrane fusion and protein decondensation take place with optimal timing. Ca^{2+} might then trigger decondensation in the same way by precipitating phosphate ions (as it does in vitro) and, indeed, such precipitates (again yielding Ca and P signals in x-ray spectra) can be recognized *in situ* under trigger conditions. As decondensation is a unidirectional, rapid process in *Paramecium* cells, it would contribute to drive the discharge of the secretory contents to the outside. Further implications on the energetics of exocytosis are discussed.

A *Paramecium* cell contains several thousand specialized secretory vesicles ("trichocysts") that can be expelled more or less synchronously by exocytosis (2, 15, 28, 35). An exocytic opening is formed by fusion of the trichocyst membrane with the cell membrane. During exocytosis the paracrystalline, periodically arranged secretory matrix proteins undergo an explosive decondensation process. The discharge of trichocysts is easily recognized in the light microscope because the organelle stretches to several times its original length; in the electron microscope the period of the matrix protein increases in a similar way (16, 17).

Both membrane fusion and matrix decondensation appear to be synchronized during exocytosis, for which the present work presents some arguments.

Recently, it became possible to isolate membrane-free trichocyst contents in the condensed state (3, 28) and to mimic in vitro the condensed → decondensed transition. We have tried to determine the relevant parameters for this step. The data obtained bear energetic aspects, ionic requirements, and timing of the final steps of exocytosis.

MATERIALS AND METHODS

Cell Material

Paramecium tetraurelia, strain K 401, was cultivated at 25°C in a monoxenic salad extract ("dried lettuce medium"; Difco Laboratories, Detroit, Mich.), with *Enterobacter aerogenes* added, and harvested at early stationary phase. The ionic conditions were as indicated elsewhere (36). Cells were concentrated and freed from bacteria and discharged trichocysts by filtration (tube with 30-μm sieve plate) and washed with a 100-fold excess of 10 mM Tris-maleate buffer, pH 7.0.

Isolation of Condensed Membrane-free Trichocysts

ISOLATION AT 2°C (METHOD A): The method is a variation of that proposed by Anderer and Hausmann (3). Cells were washed in 50 mM Tris-maleate buffer, pH 7.0 (+ 3 mM EDTA + 1.5 mM Tris-ATP), adjusted to 2°C for 1.5–2 h and then homogenized (0°C, Teflon pestle with ~0.25 mm clearance, ~15 times at ~200 rpm). The homogenate was centrifuged twice (10 min × 4,000 rpm) with a Heraeus Christ Minifuge 2 with a swing-out rotor (type 6000). The supernates were discarded. The pellet was resuspended in 1.5 ml of the above medium and layered on top of the following sucrose gradient: 6 ml of 2.1 M sucrose, 4 ml of 1.8 M sucrose, and 3 ml of 1.3 M sucrose (10 mM Tris-maleate + 3 mM EDTA + 1.5 mM Tris-ATP, pH 7.0; 2°C; glass tubes of 20 mm

THE JOURNAL OF CELL BIOLOGY · VOLUME 88 JANUARY 1981 179-188

diameter). After centrifugation (2 h × 1,500 rpm), condensed trichocysts were found in the 1.3/1.8 M sucrose interface and then washed with a 100-fold excess of buffer as used for homogenization. Electron microscope control showed almost 100% condensed trichocysts without a membrane and only little contamination by cilia, pellicles and bacteria (see reference 28). Gradients were also made with compounds other than ATP (see Table II).

ISOLATION AT 22°C (METHOD B): Cells were suspended for 30 min at 22°C in 10 mM Tris-maleate buffer with 3 mM EDTA and homogenized (see above). The homogenate was centrifuged for 10 min × 4,000 rpm; the pellet obtained was resuspended in 1.5 ml of 50 mM Tris-maleate, pH 7.0, with 3 mM EDTA added and layered on top of a discontinuous sucrose gradient (7 ml of 2.1 M, 4 ml of 1.8 M, 3 ml of 1.3 M sucrose in 3 mM EDTA + 10 mM Tris-maleate, pH 7.0). Centrifugation was carried out (2.5 h × 1,400 rpm), and condensed trichocysts were collected from the 1.3/1.8 M sucrose interface.

According to electron microscope analyses, the resulting fraction is equivalent to that obtained with the previous method.

EGTA can be used throughout procedure *A* or *B* instead of EDTA; negative pressure during homogenization has to be carefully avoided.

CRUDE TRICHOCYST-ENRICHED FRACTION BY CELL LYSIS WITH EGTA (METHOD C): Cells (~10^5/ml culture medium) were suspended in an equal volume of 8 mM EGTA in 20 mM Tris-maleate, pH 7.0, and kept at 22°C over night. All structures were destroyed except for the condensed trichocysts (contents), mitochondria, and some cytoskeletal elements. These samples contained 30 μM phosphate and 0.1 mM calcium and 0.1 mM magnesium (see reference 36). They were used only for microscopical analyses.

Isolation of Pellicles

The method used was according to Matt et al. (28).

Assay of Condensed or Decondensed State of Trichocysts

A Reichert (Austria) light microscope, type Diavar, equipped with a Nomarski interference contrast optical system, was used to monitor the state of condensation of trichocysts (i.e., their contents). The capability of various agents to produce decondensation was tested by adding an equal volume of the test solution to isolated trichocysts on a microscope slide (see Table II). The capability of various cations to precipitate phosphate from an $H_2PO_4^-/HPO_4^{2-}$ buffer under the conditions used for trichocyst decondensation was ascertained by simple test-tube experiments. Enzyme preparations added were tested spectrophotometrically for their activity.

Enzyme Assays

For the assay of Ca^{2+}-ATPase (i.e., Ca^{2+}-activated adenosinetriphosphate phosphohydrolase [EC 3.6.1.3]), the conditions were: 22°C, pH 7.8; 100-μl sample (≦100 μg of protein) added to 500 μl of 50 mM Tris-maleate + 3 mM KCl + 3 mM EDTA + 1 mM Tris-ATP (Sigma Chemical Co., St. Louis, Mo.) + $CaCl_2$. Free [Ca^{2+}] was adjusted to various concentrations with the use of a Ca^{2+}-selective electrode (calcium selectrode, model F 2112 Ca, Radiometer, W. Germany) before and after ATP was added.

The common ATPase inhibitor *p*-chloromercuribenzoate, the mitocondrial ATPase inhibitor oligomycin (25), KF as an acid phosphatase inhibitor (10, 22) and as an adenylate cyclase stimulator (see reference 45), and L-tartrate as an acid phosphatase inhibitor (31) were added 5 min before and during the assay.

The P_i released was determined as described below.

Phosphate Determinations

FREE PHOSPHATE: The method of Taussky and Shorr (44) was used. 5% TCA was added as used for protein precipitation in cell fractions.

TOTAL PHOSPHATE: The total phosphate concentration was determined according to Bartlett (5). Incineration was performed at 160°C with the addition of 10 N H_2SO_4 (3 h) and 2 drops of 30% H_2O_2 (1 h) to ≦1-ml samples (or standards).

Protein Assay

Samples were precipitated with an equal volume of 10% cold TCA, kept for 2 h at 2°C, and centrifuged (10 min × 4,000 rpm) (Heraeus Christ Minifuge 2, swing-out rotor). The sediment was hydrolyzed for ≧1 h at 22°C with 0.4 N NaOH. The method of Lowry et al. (26) (with bovine serum albumin standards) was used.

SDS-PAGE

We used the method of Fairbanks et al. (14). Isolated trichocysts were solubilized by brief heating to 100°C in the presence of 2% mercaptoethanol, 2 h before application to 8% acrylamide gels. Some gels were run without mercaptoethanol; accordingly, "trichynin" peaks were found around ~17,000 or 37,000 daltons (42). (For a definition of trichynin, see the second paragraph of *Discussion*.) Gels were usually stained with Coomassie Blue, but some gels were sliced without staining (for P_i-determination). For further details, see Bilinski et al. (7).

Production of Electron-dense Precipitates in Trichocysts In Situ

Two methods were used. (*a*) Fixation with up to 2.5% glutaraldehyde plus up to 50 mM $CaCl_2$ added; (*b*) pretreatment with ionophores X-537 A or A 23187 followed by addition of $CaCl_2$ and fixation, before massive exocytosis started, with 6.25% glutaraldehyde. Osmium tetroxide was omitted. For further details, see Plattner and Fuchs (34). With both methods, a certain fraction of resting or just discharging trichocysts displayed electron-dense deposits that were analyzed by x-ray microanalysis (see below).

Electron Microscope Analyses

ULTRASTRUCTURAL ANALYSIS: For freeze-fracturing, negative staining, and ultrathin sectioning, standard techniques were applied as before (28). Samples were viewed in a Zeiss EM 10 (80-kV, 30-μm objective aperture).

SCANNING TRANSMISSION ELECTRON MICROSCOPY AND ENERGY-DISPERSIVE X-RAY MICROANALYSIS (EDXMA):[1] Condensed or decondensed trichocysts, isolated at 22°C in a phosphate-free medium, were spread on collodion-coated Cu-grids and frozen in propane and freeze-dried at −100°C under high vacuum with a Leybold-Heraeus freeze-drier, model GT 1. During carbon coating (~25 nm), samples were permanently tilted and rotated on a special holder of the Leybold-Heraeus evaporator EPA 100. 200-nm sections of cells with electron-dense deposits in trichocysts (see above) were treated in a similar way.

The samples were further analyzed with a Zeiss EM 10C electron microscope in the scanning transmission mode (STEM) under the following conditions: acceleration voltage, 40 kV; beam current, ~50 μA; probe diameter, ~15 nm; magnification, × 10^4; top entry cartidge with a carbon fixing; 30-mm^2 Kevex Li-Si detector with collimator; 8-μm Be window; window-sample distance, 25 mm; fixed 45° tilting; Kevex spectrometer unit 7000. The Cu-Kα and Lα lines were used for calibration. 100-s point measurements were made. The Si-Kα signals are an artifact (see reference 41).

MICROPROBE ANALYSIS: Pellets of freshly isolated, hydrated trichocyst fractions in the condensed state or after in vitro decondensation were put onto aluminum SEM-holders and mounted under LN_2 onto a massive aluminum block that, in consecutive steps, was transferred under LN_2 into a vacuum evaporation unit for carbon coating (25 nm) and then into the microprobe SEM unit for analysis. In both cases the evacuation time was short enough to keep the temperature sufficiently low. Evaporation or microprobe analysis, respectively, was started when the specimen surface began to defrost. Freeze-dried aliquots were also analyzed.

A microprobe unit, type SEM Q, from Applied Research Laboratories (ARL, Los Angeles, Calif.) was used. Operation conditions: secondary electron scanning mode (SEM); acceleration voltage, 20 kV; beam current, 0.5 μA; probe diameter, 20 nm; sample current, 10 nA; magnification, × 10^3. X-ray energies were recorded with a Kevex detector (system 5000; Li-Si crystal; 100 mm^2 frontal area; take-off angle, 55°; sample detector distance, 50 mm; 0.2 mm Be window; counting time, 1 min) and data processor (system 6000). For high-energy resolution, the P-Kα_1 and S-Kα_1 lines were scanned with a pentaerythrol crystal of the ARL scanning spectrometer unit.

RESULTS

The secretory contents of *Paramecium* "trichocysts" were isolated by different methods. The dissociation from the surface membrane complex ("pellicles"), to which trichocysts adhere *in situ* by their membrane envelope, was monitored by mea-

[1] *Abbreviations used in this paper:* AIDP, adenosine imidodiphosphate; EDXMA, energy-dispersive x-ray microanalysis; GTP, guanosine triphosphate; LN_2, liquid nitrogen; PAGE, polyacrylamide gel electrophoresis; P_i, inorganic phosphate; SEM, (secondary electron) scanning electron microscope; STEM, scanning transmission electron microscope.

surements of the Ca^{2+}-ATPase activity characteristic for pellicles (7). Only ~0.1 of the specific activity of pellicles was found in trichocyst fractions. Various ATPase and phosphatase inhibitors (Table I) did not inhibit the Ca^{2+}-ATPase activity of pellicles and the small activity in trichocyst fractions, whereas *p*-chloromercuribenzoate inhibited Ca^{2+}-ATPase in both fractions to the same degree (Table I). This, in conjunction with SDS-PAGE results (7), indicates that the residual Ca^{2+}-ATPase in trichocyst fractions might be attributable to a minor contamination by pellicles.

Isolated trichocysts show the same ultrastructural elements (Fig. 2) as *in situ* trichocysts; only the outer sheath, a minor structural element of the "tip" portion (see reference 4), and the membrane envelope are absent. This was documented in more detail in a previous paper (28). The decondensation process can be analyzed in vitro with isolated trichocyst fractions; it can be followed by light (Fig. 1) or electron microscope (Figs. 2–5) methods. Upon decondensation, which involves exclusively the paracrystalline matrix of the "body" ("matrix") portion, a 57-nm periodicity becomes visible with all electron microscope preparation methods used (Figs. 3–5). This period is almost 10 times larger than that in condensed trichocysts, which is visible only under favorable conditions. Concomitantly, each trichocyst expands to about five times (the matrix about 10 times) its original length during decondensation. The process is the same as during trichocyst exocytosis.

In Table II, trichocyst fractions were used from slightly different isolation procedures; it is especially difficult to keep the trichocyst proteins in the condensed state during isolation close to 0°C. Isolation method *A* was used as previously described (see references 3 and 28) and reused with different variations in the present paper, because we intended to show that it is not the concentration of ATP or of other nucleotides added but solely a critical concentration (≧10 μM) of free, ionized phosphate, which accounts for maintaining trichocysts in the condensed state. Method *B* was designed because we found that the chelation of the endogenous Ca^{2+} by EGTA during homogenization and presumably the higher solubility of the endogenous P_i content at ambient temperature (and/or other factors unknown to us) are evidently sufficient to keep trichocysts condensed during the whole isolation procedure. The latter method is especially important, because it allows one to measure the endogenous P_i content without the addition of an excess of exogenous P_i. After both isolation procedures,

TABLE I

Response of Ca^{2+}-ATPase Activity in Trichocysts and Pellicles to [Ca^{2+}] and to Inhibitors *

	Trichocysts (A)	Pellicles (B)	A/B
0.3 mM Ca^{2+}	25	213	0.12
0.9 mM Ca^{2+}	52	388	0.13
1.8 mM Ca^{2+}	75	544	0.14
p-Chloromercuribenzoate	10	120	0.08
Oligomycin (50 μg/ml)	75	533	0.14
KI	72	Not done	—
KF	73	Not done	—
L-Tartrate	71	Not done	—
L-Tartrate + KI + p-Cl-mercuribenzoate	4	Not done	—

* Expressed in nmol P_i/mg protein per min. 1 mM ATP and 5 mM inhibitors added (except for oligomycin). The free Ca^{2+} concentration was 1.8 mM, except where indicated otherwise. The experiments were conducted at 22°C.

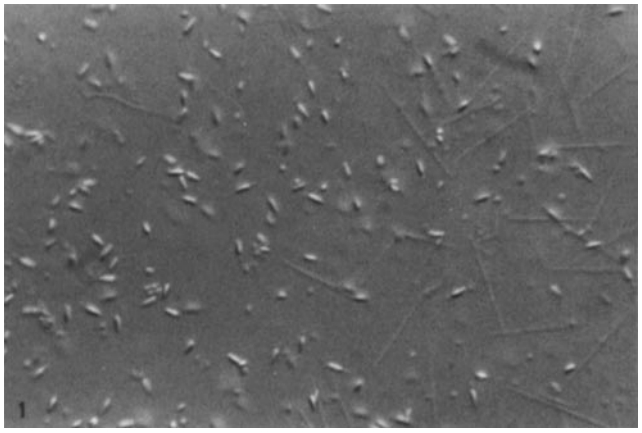

FIGURE 1 Nomarski interference contrast micrograph from a trichocyst-enriched fraction. On the left, trichocysts are in the condensed state; calcium chloride was added on the right side and decondensation takes place along the diffusion front. × 900.

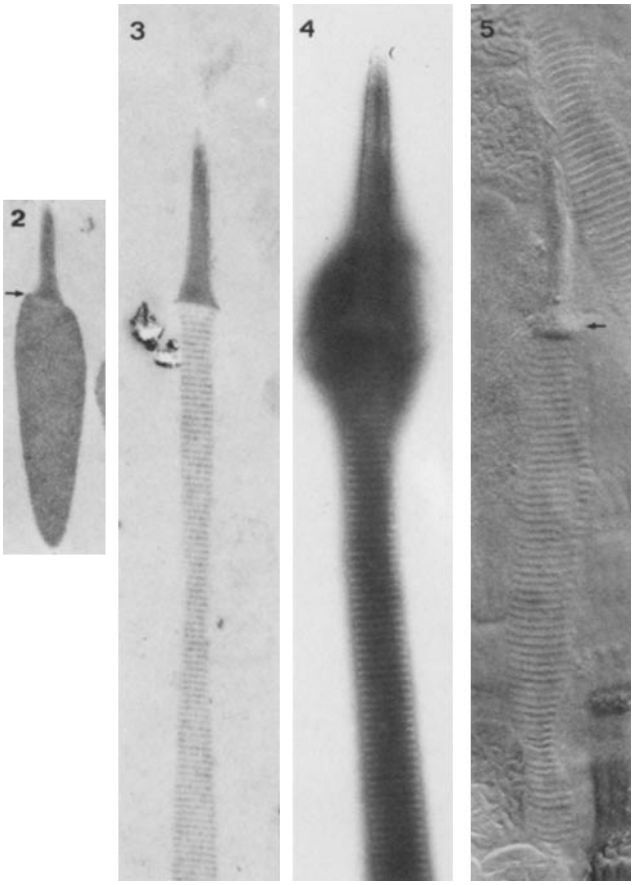

FIGURES 2–5 Electron micrographs from isolated trichocysts (method A). Note the absence of a membrane (as shown in more detail previously [28]), the presence of the matrix in a condensed (Fig. 2) or decondensed state (Figs. 3–5) and an unaltered tip portion, containing a paracrystalline core and the surrounding "inner lamellar sheath" (see Anderer and Hausmann [3], Bannister [4], and Matt et al. [28]). With all electron microscope methods used, the period in the decondensed state is ~57 nm. The arrows mark the limits between "tip" and "body" (matrix) region. Figs. 2 and 3 are ultrathin sections; Fig. 4 is a negative staining sample; Fig. 5 is a freeze-fracture replica. × 19,000.

TABLE II

Condensation → Decondensation Transition in Trichocysts in Vitro

Isolation medium*	Compounds added after isolation	State of condensation
A. 2°C, 1.3 M sucrose + 3 mM EDTA or EGTA + ATP (or ADP, AMP, GTP, AIDP‡, or KH_2PO_4) in 20 mM Tris-maleate buffer, pH 7.0		
(1) Free $P_i \geq 10^{-5}$ M	—	Condensed
(2) Free $P_i \leq 10^{-5}$ M	—	Decondensed
(3) $-P_i$, + 10^{-3} M adenosine	—	Decondensed
(4) $-P_i$, + 5 mM NaH_2AsO_4	—	Decondensed
(5) − EDTA or EGTA, + $>10^{-5}$ M free P_i	—	Decondensed
(6) Like *1*	$\geq 10^{-4}$ M tertiary amines or Ca^{2+}§	Decondensed
(7) Like *1*	Excess of buffer	Decondensed
(8) Like *1*	Isolation medium-sucrose (different phosphates with free $P_i \geq 10^{-5}$ M)	Condensed
B. 22°C, 4 mM EGTA in 20 mM Tris-maleate buffer, pH 7.0 (containing 30 μM free P_i)		
(1) Medium *B*	—	Condensed
(2) Like *1*	10 × diluted with buffer + EGTA	Decondensed
(3) Like *1*	Acid or alkaline phosphatase, K^+,Na^+-ATPase	Condensed
(4) Like *1*	5 mM solution of:‖	
	Ca^{2+}, Cu^{2+}, Pb^{2+}	Decondensed
	Ag^+, Cd^{2+}, Sn^{2+}	Partly decondensed
	K^+, Na^+, Mn^{2+}, Ba^{2+}, Sr^{2+}, Hg^{2+}, Bi^{2+}, Ni^{2+}, Li^{2+}	Condensed
(5) Like *1*	Tertiary amines, ~1 mM§	Decondensed
(6) Like *1*	Centrifugation → resuspension in:	
	Mg^{2+}, 1 mM, in EGTA buffer	Condensed
	Mg^{2+}, 0.1 mM, in EGTA buffer	Decondensed

* 0.5 × diluted if compounds were added after isolation.

‡ Free, hydrolyzed phosphate concentrations were 4.7, 3.9, 0.6, 7.6, and 3.7% (wt/wt), referring to the terminal phosphate group, for ATP, ADP, AMP, GTP, and AIDP, respectively.

§ Dibucaine, chlorpromazine. These compounds were found to precipitate P_i in the given concentrations.

‖ All salts except for Ag^+ (nitrate) and Pb^{2+} (citrate or nitrate) were chlorides, pH 7.0.

all trichocysts can be recovered in the condensed state and then decondensed by P_i precipitation (Table II).

With method *A*, various nucleotides can conserve the condensed state only when their hydrolysis rate yields a free $[P_i] \geq 10$ μM and, thus, do not seem to be protective on their own. Structurally related anions, such as AsO_4^{3-}, cannot substitute for P_i. A variety of cations, such as Ca^{2+}, Pb^{2+}, and Cd^{2+}, which precipitate P_i, result in decondensation (Table II *B-4*), whereas other cations, such as K^+, Na^+, and others, remain without effect. Decondensation is also achieved with tertiary amines (Fig. 1; Table II *B-5*). Mg^{2+} (its phosphate being soluble) in millimolar concentration acts as an inhibitor for decondensation. Other components used for isolation, such as buffer salts and sucrose, do not interfere. Table II also shows that exogenously added alkaline or acid phosphatase (~10 mU/assay) or solubilized ATPase preparations do not lead to decondensation. The latter is an argument against the earlier assumption (3, 28) of an involvement of ATP in maintaining the condensed state.

Therefore, it appeared plausible to look for ionically bound P_i and, possibly, for Mg^{2+}, which could prevent trichocyst "matrix" proteins from undergoing the condensed→decondensed transition. This was done by chemical determinations of the P_i content and by EDXMA spectral recordings from isolated trichocysts.

According to Table III, a considerable concentration of P_i is bound to trichocysts; most of it is in the form of free P_i and, thus, released by TCA. Results with gel slices rule out protein phosphorylation. Although it can not be excluded on the basis of Table III that a small fraction of phosphate could be in a

TABLE III

Phosphate Content of Isolated Cell Fractions *

Sample	Free phosphate‡	Total phosphate§
Homogenate	411	
Pellicles	0	
Trichocyst contents		
Condensed	230 (Supernatant)	279 (232 protein bound, 47 supernatant)
	286 ‖ (Supernatant)	
Decondensed	212 (Supernatant)	308 (241 protein bound, 67 supernatant)
Trichynin band of electrophoreses	0	0 Found (expected to be 10 × above background)¶

* All values are expressed as nmol/mg protein; for protein-free supernates values refer to the corresponding protein in pelleted trichocysts. Trichocysts were isolated in a phosphate-free medium at 22°C (method *B*) except for entry marked with ‖.

‡ 5% TCA precipitation.

§ Incineration method of Bartlett (5).

‖ Isolated at 2°C with a medium supplemented with 1.5 mM Tris-ATP (containing 71 μM free hydrolyzed phosphate). Samples were washed with a phosphate-free medium before TCA precipitation and phosphate determination.

¶ From SDS-polyacrylamide gels obtained from heat- and mercaptoethanol-solubilized isolated trichocysts, the 1-cm-long 15- to 20-kdalton region (including the ~17-kdalton trichynin peak) was cut out and incinerated. The total phosphate content was within the background fluctuations found within other gel regions or within a blank gel (~15 nmol/cm gel). The expected value is calculated from the amount of protein used and from the intensity distribution in parallel Coomassie Blue-stained gels.

form other than orthophosphate, this seems unlikely to be relevant for the maintenance of the condensed state on the basis of Table II. Interestingly, decondensation does not result in a rapid release of P_i; the resulting precipitate seems to be adsorbed to the protein. This corresponds to the situation observed with EDXMA recordings after isolation as well as *in situ* (see below), which both show that the precipitate formed becomes adsorbed to the decondensed trichocyst.

EDXMA recordings from hydrated (Figs. 6 and 7) or freeze-dried (Figs. 10 and 11) pellets or freeze-dried single trichocysts (Figs. 13 and 15) showed quite similar P signals. These analyses rule out artifacts attributable to element redistribution or—when single trichocysts were analyzed—to contaminants. The SEM morphology was registered to monitor the occurrence of the condensed→decondensed transition (Figs. 8 and 9). The same holds true for STEM micrographs of single trichocysts (Figs. 14 and 16). Fig. 12 is a wavelength-dispersive recording for unequivocal identification of P-Kα_1 and S-Kα_1 signals. The latter indicates the presence of cystein (see reference 42). The different texture of condensed or decondensed samples does not allow for a direct calculation of P content to S content. Both elements occur also in the trichocyst tip (Figs. 13–16). Mg signals were obtained only from the condensed trichocyst matrix. It appears therefore possible that Mg is released upon decondensation.

These results are in line with EDXMA recordings from trichocysts *in situ*. When cells are exposed to Ca^{2+} ionophores (see reference 34), electron-dense deposits are frequently found in "activated" (not yet discharging) or discharging trichocysts (Fig. 17); this precipitate is lost from completely discharged trichocysts. Apparently, the fixation process does not allow for diffusion from within the cell. The precipitates thus formed display P and S signals in EDXMA spectra (Figs. 18 and 19).

A possible summary of events is presented in Fig. 20.

DISCUSSION

It is economical for a cell to pack its exportable proteins into containers that are as small as possible and to decondense them only at the moment of release. For the performance of dis-

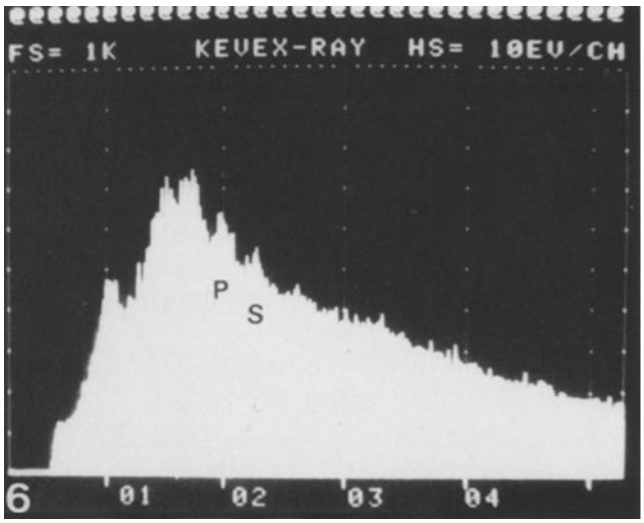

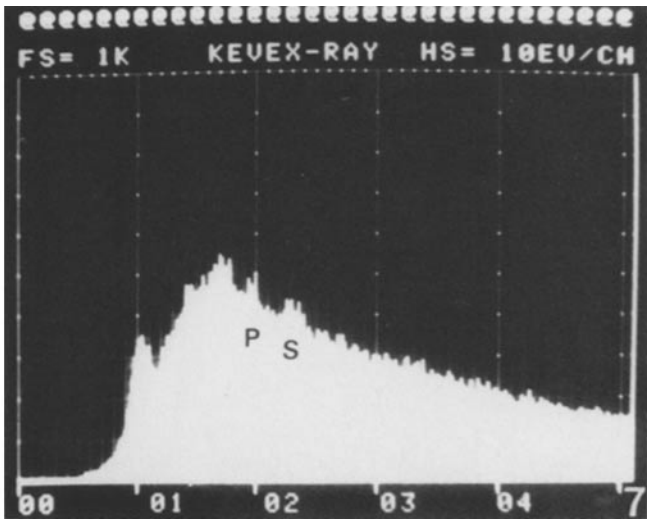

FIGURES 6 and 7 EDXMA spectra recorded from pellets of isolated trichocysts in the hydrated state (isolation method B; C-coating and analysis on cold stage). Fig. 6: condensed state; Fig. 7: after decondensation by dibucaine.

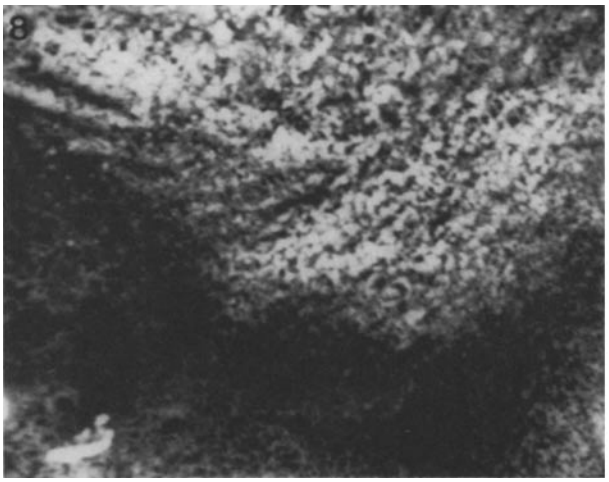

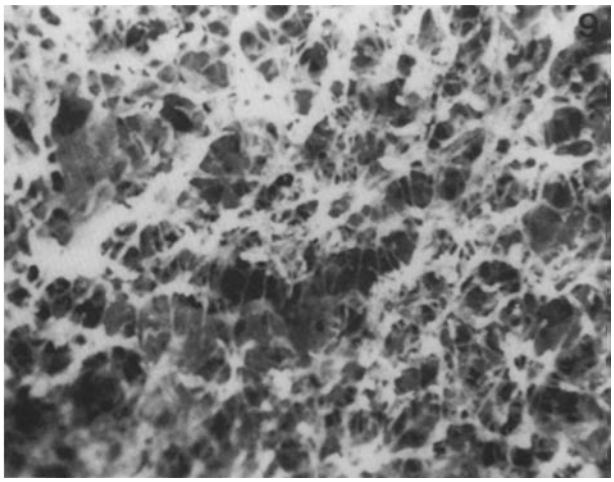

FIGURES 8 and 9 Loosely packed trichocyst fractions (isolated by method B) frozen, freeze-dried, C-coated, and analyzed in the microprobe device. Despite the inferior imaging quality of these SEM pictures, both micrographs allow one to ascertain the condensed state (Fig. 8) and the dibucaine-mediated decondensation (Fig. 9) in relation to the corresponding EDXMA spectra presented in Figs. 10 and 11. × 900.

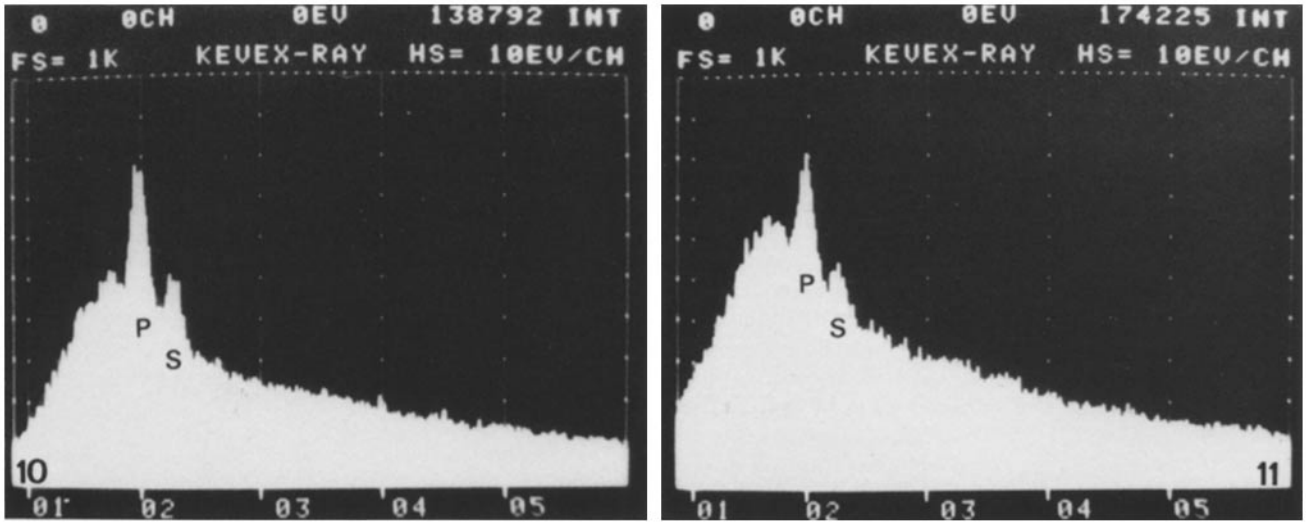

FIGURES 10 and 11 EDXMA spectra recorded from the freeze-dried trichocyst pellets depicted in Figs. 8 and 9. Fig. 10 is from condensed, Fig. 11 from decondensed trichocysts.

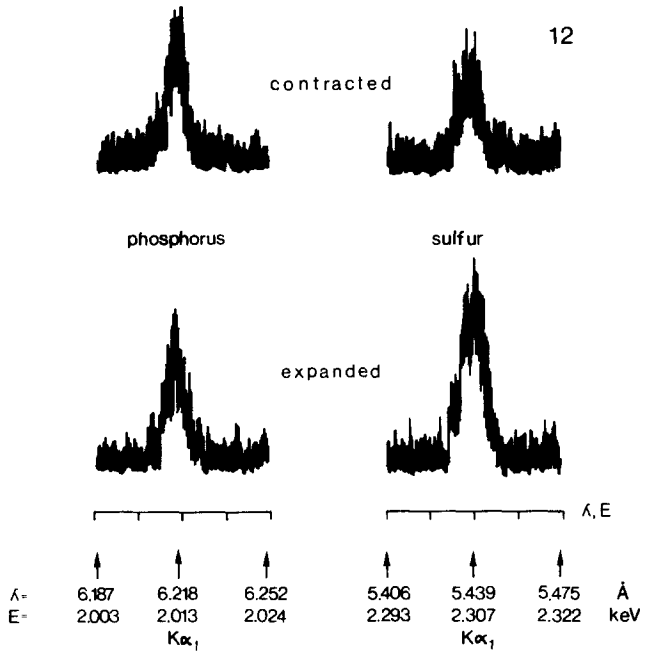

FIGURE 12 Wavelength-dispersive scans for identification of P-Kα_1 and S-Kα_1 peaks. The scans were obtained from the same freeze-dried trichocyst samples as in Figs. 8 and 9 and Figs. 10 and 11. "Contracted" indicates the condensed, "expanded" the decondensed, state of trichocysts.

charge, several mechanisms could be taken into account, but we present here some evidence for our particular system that unidirectional decondensation of trichocyst proteins drives their own discharge. The mechanism proposed operates by a change of the ionic conditions within the secretory granule, once exposed to the extracellular environment (high Ca^{2+}) after the formation of an exocytic opening (Fig. 20). This explains also the precise timing of these events during exocytosis.

Characteristics of the Secretory Contents of Paramecium Trichocysts

Trichocysts have a minor "tip" portion and a massive "body" ("matrix") portion (Figs. 2–5); only the latter undergoes decondensation during discharge (4). In SDS-PAGE scans of trichocyst contents there occurs a massive broad band around ~36,000 or ~17,000 daltons (with mercaptoethanol) (42). Gels with higher resolution show that these trichynin bands represent a "family" of similar proteins; upon isoelectric focusing, trichynins show up predominantly as slightly acidic and less as slightly alkaline polypeptides (1). It has also long been known that these periodic proteins undergo decondensation (Fig. 2–5) upon discharge with a considerable increase in size, both of the trichocyst body as a whole and of its periodicity (16–18).

Decondensation of Secretory Materials in Paramecium and in Other Systems

The process of exocytosis is generally considered independent of the kind of secretory materials released (32). Such materials are frequently proteins, especially glycoproteins (see references 29 and 32), but some exocytic systems, such as acetylcholine transmitter vesicles, contain only nonprotein materials (43, 47). Secretory vesicles involved in catecholamine secretion contain acidic proteins, besides Ca^{2+} and ATP, that counterbalance surplus charges (48). The presence of sulfated compounds in some secretions (8, 39) might exert a similar effect. In addition, the high Ca^{2+} content in different secretions (11, 27) can also screen excess charges. We here report on the absence of Ca^{2+} and probably of ATP and on the presence of P_i ions in the particular secretion analyzed.

In conclusion, there is no general rule for the occurrence of proteins (or of special charge types) or of certain ions in secretory materials. We found with our particular systems that compositional aspects of secretory contents have some bearing on the decondensation process and, concomitantly, on the mechanism of exocytosis (see below).

In other systems, the secretory materials look normally amorphous in the electron microscope. However, closer inspection revealed regular substructures also in insect gland (37), salivary gland (40, 46), pancreatic zymogen (13), mast cell (9), and sea urchin egg cortical granules (6). The occurrence of a clear paracrystalline structure in secretory materials can be observed only occasionally in various exocrine granules (e.g., glucagon storage vesicles; see reference 24), whereas this is the rule in protozoan "extrusomes", such as trichocysts (2, 15).

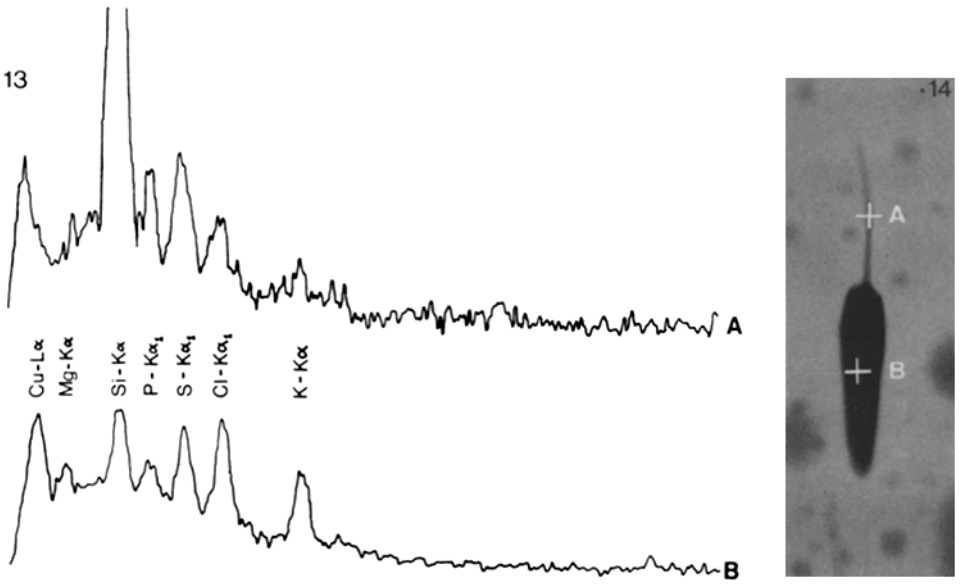

FIGURES 13 and 14 STEM analysis of an individual condensed trichocyst (isolation procedure B, freeze-drying, and C-coating). Fig. 13 presents the EDXMA spectra recorded from the positions indicated on Fig. 14, i.e., tip and matrix. Fig. 14, × 5,900.

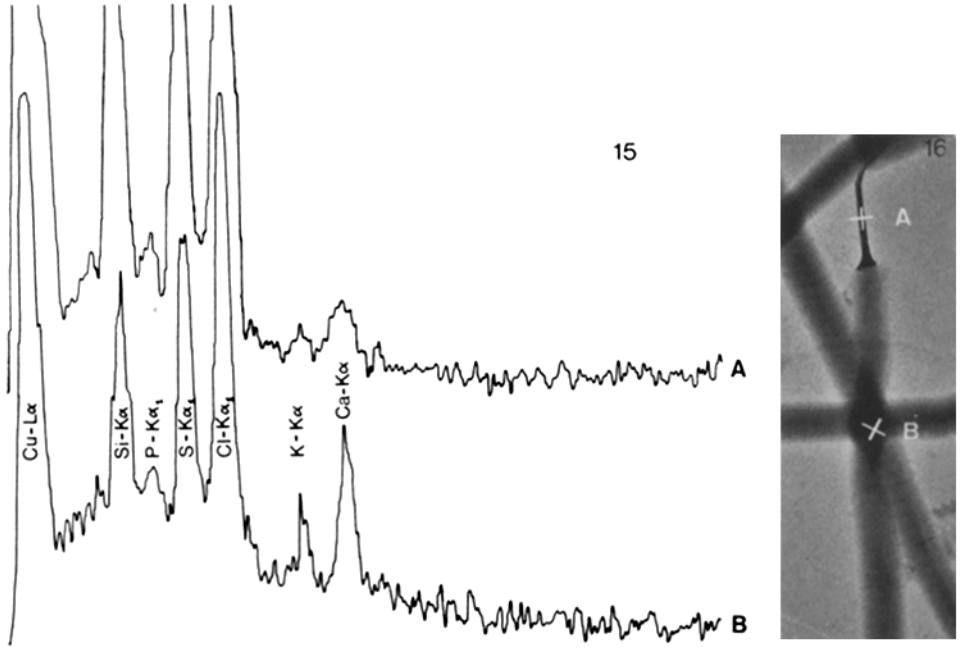

FIGURES 15 and 16 Same situation as in Figs. 13 and 14, but for a trichocyst decondensed by addition of $CaCl_2$ before freezing and drying. Fig. 16, × 5,900.

The decondensation time for trichocysts was estimated to be less than a few milliseconds (33)—according to high-speed cinematographic results, probably 0.5 ms (Plattner, Bilinski, and Völlenklee, unpublished observations). Surprisingly, the discharge time for mast cell granules is also in the millisecond range (12), so that exocytosis might be in different systems a more vigorous process than commonly assumed. Moreover, quite similar to *Paramecium* trichocysts, mast cell secretory granules (9, 20, 23), oocyte cortical granules (6), and other secretory granules (29) also undergo a decondensation process, visible as a decrease in electron contrast, during exocytosis. These arguments also favor the assumption that decondensation is a more common phenomenon that might facilitate the release of secretory protein.

Mechanism Proposed for Protein Decondensation in Paramecium Trichocysts

The mechanism proposed is summarized in Fig. 20, based on the results with different isolation media (Table II), of P_i determinations (Table III) and of x-ray recordings from isolated trichocysts (Figs. 6–16). The evidence given in Results shows that phosphorus is predominantly, if not exclusively, ionically bound as P_i to the trichocyst protein. P_i is assumed to maintain the condensed state by screening excess charges. Unfortunately, the isoelectric points are less relevant for this aspect, and the tertiary structure of trichynins and their mutual arrangement are not yet known. Nevertheless, electron stains of different charges selectively stain some substructures of the

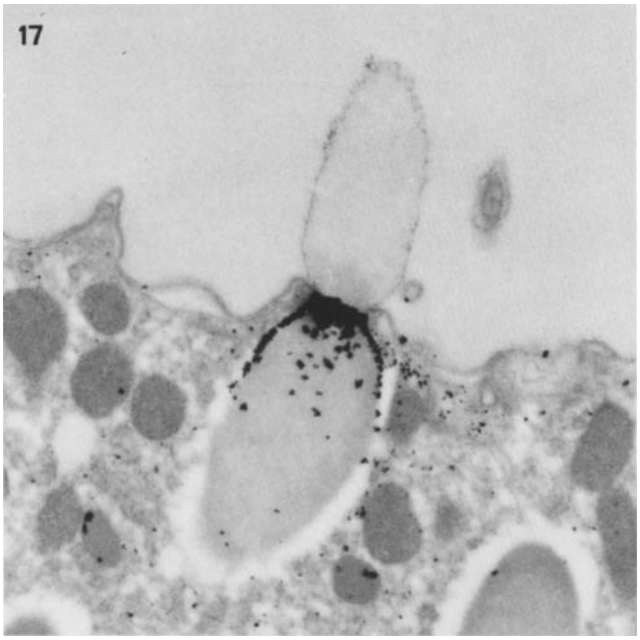

FIGURES 17–19 Electron-dense deposits produced within a trichocyst *in situ* as indicated in Materials and Methods; Fig. 17 shows the transition between the condensed and the decondensed states of a trichocyst matrix ("body"). Fig. 19 is a STEM x-ray energy recording from a deposit similar to that in Fig. 17. Fig. 18 indicates the "preparative" background lines of Cl (from embedding medium) and Cu (from support grid), which have to be subtracted from Fig. 19. Fig. 17, × 18,000.

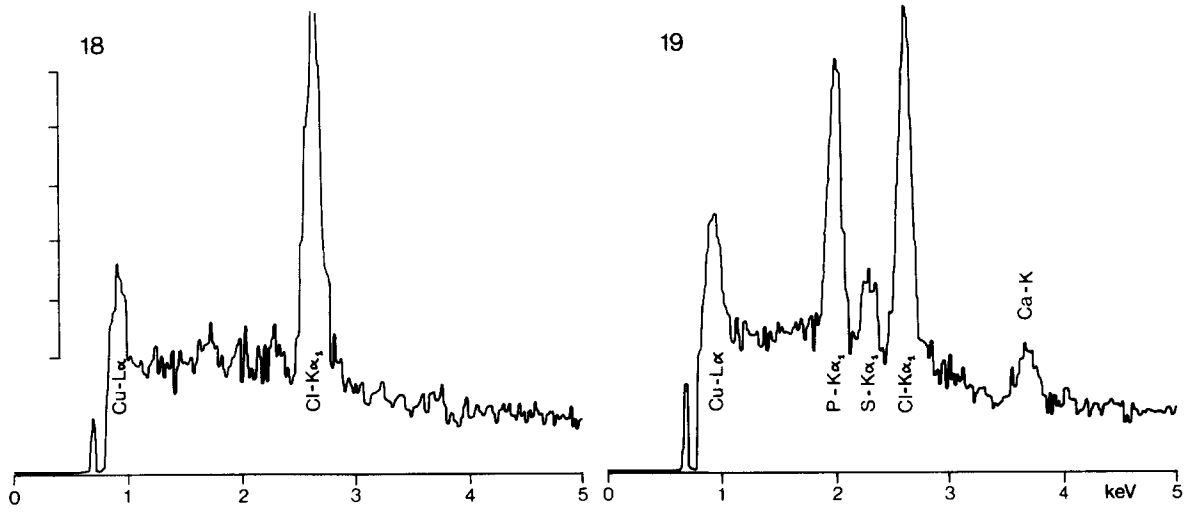

trichocyst matrix (Westphal and Plattner, unpublished observations), indicating a complicated framework for ionic interactions.

In Fig. 20, we propose that the high external [Ca^{2+}], which gains access to the secretory contents via the exocytic canal, precipitates P_i and that this entails decondensation. The occurrence of Mg signals in EDXMA indicates a possible role of Mg^{2+} for maintaining the condensed state *in situ*; this is underscored by the inhibitory effect of Mg^{2+} in vitro. These arguments are corroborated by the widely different solubilities of magnesium and calcium phosphates. When compared with the excess positive charges to be expected from the amino acid composition of trichynin (42), a balance calculation shows that this figure is equivalent to the minimal [P_i] required to maintain the condensed state. According to Tables II and III, it is unlikely that nucleotides or other phosphates or protein phosphorylation would contribute to condensation. Previously, ATP had been considered necessary to keep trichocysts in the condensed state (3, 28); the findings presented here show that a certain level of free hydrolyzed P_i is sufficient to avoid decondensation. This is in accordance with our finding that various P_i precipitating cations (including some inorganic and organic cations) can evoke decondensation in vitro (Table II). As far as the decondensating effect of tertiary amines (local anesthetics) is concerned, it agrees with the generally known capacity of these agents to substitute for Ca^{2+} (see reference 28).

According to the presence of cystein groups (42), which accounts for the S-Kα_1 signals in EDXMA scans (Figs. 6–16), sulfhydryl groups might be involved in the regulation of the state of condensation in an as yet unknown way. The lack of any effect of added phosphatase or ATPase preparations (Table II) and of endogenous enzyme activities (from a minor contamination with pellicle membranes) is in line with the assumption that decondensation is a nonenzymatic effect. This might be necessary to account for the rapidity of this process.

General Conclusions

The final steps of exocytosis are considered to be energy (ATP)-dependent in general (19, 32) and in *Paramecium* cells in particular (28). It is now important to pinpoint the individual

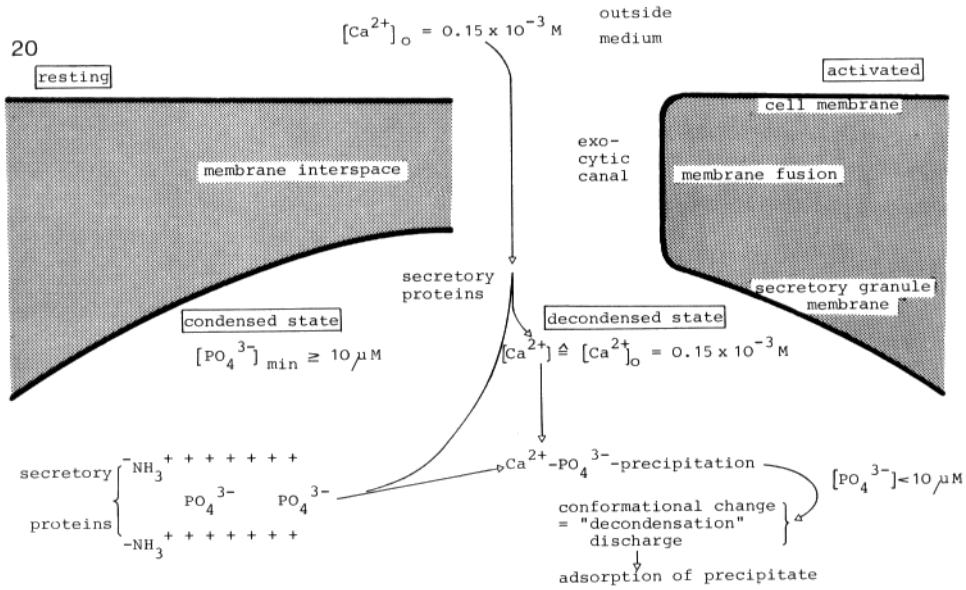

FIGURE 20 Conclusions on possible ionic interactions that lead to the decondensation of secretory proteins in *Paramecium* trichocysts. P_i is thought to screen positive charges of secretory proteins, which, at least in part, are attributable to free amino groups. The scheme does not account for the possible screening of negative charges of condensed proteins by Mg^{2+}. *Left*, resting state; *right*, activated state after formation of an exocytic canal. For further explanations, see text.

energy-requiring steps. From the results presented here, one must conclude that decondensation does not consume energy, although decondensation could be a driving force for the discharge of trichocysts. The energy for discharge by decondensation has been provided at earlier steps during organelle biogenesis. We do not know yet the specific energy requirements for other steps involved in the whole process of exocytosis of secretory products.

Because there is no general rule for the organization of secretory contents, several systems should be analyzed in this regard. The system analyzed here might appear specialized, yet it represents a most efficient "machinery" for exocytosis and, thus, might serve as an appropriate model system.

It was postulated for adrenal medullary cells (21, 38) that the equilibration of an osmotic imbalance and swelling of secretory granules leads to a vigorous discharge of the secretory contents. A mechanism of this type can not be assumed for our system because it is possible in paramecia to provoke membrane fusion without discharge of the trichocyst contents, when decondensation is inhibited at the same time (Plattner and Matt, manuscript in preparation).

We thank the following persons for their help: R. Bauer (C. Zeiss, Oberkochen, Germany), E. Huber (Inst. Pharmacol., Innsbruck, Austria), J. Klima (Lab. Electron Microscopy, Innsbruck) and E. Mersdorf (Inst. Mineralogy, Innsbruck). We also gratefully acknowledge the skillful phototechnical assistance of Mrs. D. Bliestle and E. Kiechle and the secretarial help of Mrs. U. Remensperger.

This work was financially supported by the Österreichische Forschungsfonds and the Deutsche Forschungsgemeinschaft, SFB 138.

This work was taken in part from a Ph.D. thesis by M. Bilinski; it was briefly presented at the Conference of German Societies of Cell Biology (Berlin, 1979).

Received for publication 17 March 1980, and in revised form 8 July 1980.

Note Added in Proof: While this paper was in press, Ca^{2+}-dependence of secretory protein decondensation was postulated also for mast cells (Caulfield et al., 1980, *J. Cell Biol.* 85:299–311), although on the basis of circumstantial evidence only.

REFERENCES

1. Adoutte, A., R. Ramanathan, R. M. Lewis, R. R. Dute, K. Y. Ling, C. Kung, and D. L. Nelson. 1980. Biochemical studies of the excitable membrane of *Paramecium tetraurelia*. III. Proteins of cilia and ciliary membranes. *J. Cell Biol.* 84:717–738.
2. Allen, R. D. 1978. Membranes of ciliates: ultrastructure, biochemistry and fusion. *In* Membrane Fusion. G. Poste and G. L. Nicolson, editors. North Holland Publishing Co., Amsterdam, The Netherlands. 657–763.
3. Anderer, R., and K. Hausmann. 1977. Properties and structure of isolated extrusive organelles. *J. Ultrastruct. Res.* 60:21–26.
4. Bannister, L. H. 1972. The structure of trichocysts in *Paramecium caudatum*. *J. Cell Sci.* 11:899–929.
5. Bartlett, G. R. 1959. Phosphorus assay in column chromatography. *J. Biol. Chem.* 234: 466–468.
6. Begg, D. A., and L. I. Rebhun. 1979. pH regulates the polymerization of actin in the sea urchin egg cortex. *J. Cell Biol.* 83:241–248.
7. Bilinski, M., H. Plattner, and R. Tiggemann. Isolation of surface membranes from normal and exocytotic mutant strains of *Paramecium tetraurelia*. Ultrastructural and biochemical characterization. *Eur. J. Cell Biol.* In press.
8. Blaschke, E., U. Bergqvist, and B. Uvnäs. 1976. Identification of the mucopolysaccharides in catecholamine-containing subcellular particle fractions from various rat, cat and ox tissues. *Acta Physiol. Scand.* 97:110–120.
9. Caulfield, J. P., R. A. Lewis, A. Hein, and K. F. Austen. 1979. Secretion in dissociated human lung mast cells. *J. Cell Biol.* 83 (2, Pt. 2): 432*a* (Abstr.).
10. Chakravarty, N. 1979. Correlation between plasma membrane ATPase activity of mast cells and histamine secretion. *Agents Actions.* 9:62–63.
11. Clemente, F., and J. Meldolesi. 1975. Calcium and pancreatic secretion. I. Subcellular distribution of calcium and magnesium in the exocrine pancreas of the guinea pig. *J. Cell Biol.* 65:88–102.
12. Douglas, W. W. 1974. Involvement of calcium in exocytosis and the exocytosis-vesiculation sequence. *Biochem. Soc. Symp.* 39:1–28.
13. Ermak, T. H., and S. S. Rothman. 1978. Internal organization of the zymogen granule: formation of reticular structures in vitro. *J. Ultrastruct. Res.* 64:98–113.
14. Fairbanks, G., T. L. Steck, and D. F. H. Wallach. 1971. Electrophoretic analysis of the major polypeptides of the human erythrocyte membrane. *Biochemistry.* 10:2606–2617.
15. Hausmann, K. 1978. Extrusive organelles in protists. *Int. Rev. Cytol.* 52:197–276.
16. Hausmann, K., W. Stockem, and K. E. Wohlfarth-Bottermann. 1972. Cytologische Studien an Trichocysten. I. Die Feinstruktur der gestreckten Spindeltrichocyste von *Paramecium caudatum*. *Cytobiologie.* 5:208–227.
17. Hausmann, K., W. Stockem, and K. E. Wohlfarth-Bottermann. 1972. Cytologische Studien an Trichocysten. II. Die Feinstruktur ruhender und gehemmter Spindeltrichocysten von *Paramecium caudatum*. *Cytobiologie.* 5:228–246.
18. Jakus, M. A. 1945. The structure and properties of the trichocysts of *Paramecium*. *J. Exp. Zool.* 100:457–476.
19. Jamieson, J. D., and G. E. Palade. 1971. Condensing vacuole conversion and zymogen granule discharge in pancreatic exocrine cells: metabolic studies. *J. Cell Biol.* 48:503–522.
20. Kagayama, M., and W. W. Douglas. 1974. Electron microscope evidence of calcium-induced exocytosis in mast cells treated with 48/80 or the ionophores A-23187 and X-537A. *J. Cell Biol.* 62:519–526.
21. Kirshner, N., and O. H. Viveros. 1972. The secretory cycle in the adrenal medulla. *Pharmacol. Rev.* 24:385–398.

22. Kutscher, W., and A. Wörner. 1936. Prostataphosphatase. 2. Mitteilung. *Z. Physiol. Chem.* 239:109–126.
23. Lagunoff, D. 1973. Membrane fusion during mast cell secretion. *J. Cell Biol.* 57:252–259.
24. Lange, R. H. 1979. Distribution of molecule numbers per secretion granule. A study of crystals in glucagon secreting cells. *Eur. J. Cell Biol.* 20:71–75.
25. Lardy, H. A., D. Johnson, and W. C. McMurray. 1958. Antibiotics as tools for metabolic studies. I. A survey of toxic antibiotics in respiratory, phosphorylative and glycolytic systems. *Arch. Biochem. Biophys.* 78:587–597.
26. Lowry, O. H., N. J. Rosebrough, A. J. Farr, and R. J. Randall. 1951. Protein measurement with the Folin phenol reagent. *J. Biol. Chem.* 193:265–275.
27. Malaisse, W. J., A. Herchuelz, J. Levy, G. Somers, G. Devis, M. Ravazzola, F. Malaisse-Lagae, and L. Orci. 1975. Insulin release and the movements of calcium in pancreatic islets. *In* Calcium Transport in Contraction and Secretion. E. Carafoli, F. Clementi, W. Drabikowski, and A. Margreth, editors. North Holland Publishing Co., The Netherlands. 211–226.
28. Matt, H., M. Bilinski, and H. Plattner. 1978. Adenosine-triphosphate, calcium and temperature requirements for the final steps of exocytosis in *Paramecium* cells. *J. Cell Sci.* 32:67–86.
29. Meldolesi, J., N. Borgese, P. DeCamilli, and B. Ceccarelli. 1978. Cytoplasmic membranes and the secretory process. *Cell Surf. Rev.* 5:509–627.
30. Millonig, G. 1969. Fine structure analysis of the cortical reaction in the sea urchin egg: after normal fertilization and after electric induction. *J. Submicrosc. Cytol.* 1:69–84.
31. Nelson, B. D. 1966. Rat liver acid phosphatase: differences in lysosomal and cytoplasmic forms. *Proc. Soc. Exp. Biol. Med.* 112:998–1001.
32. Palade, G. E. 1975. Intracellular aspects of protein synthesis. *Science (Wash. D. C.).* 189: 347–358.
33. Pitelka, D. 1963. Electron microscope structure of protozoa. Pergamon Press, Oxford.
34. Plattner, H., and S. Fuchs. 1975. X-ray microanalysis of calcium binding sites in *Paramecium.* With special reference to exocytosis. *Histochemistry.* 45:23–47.
35. Plattner, H., F. Miller, and L. Bachmann. 1973. Membrane specialization in the form of regular membrane-to-membrane attachment sites in *Paramecium.* A correlated freeze-etching and ultrathin-sectioning analysis. *J. Cell Sci.* 13:687–719.
36. Plattner, H., K. Reichel, H. Matt, J. Beisson, M. Lefort-Tran, and M. Pouphile. Genetic dissection of the final exocytosis steps in *Paramecium tetraurelia* cells: cytochemical determination of Ca^{2+}-ATPase activity over preformed exocytosis sites. *J. Cell Sci.* In press.
37. Plattner, H., M. Salpeter, J. E. Carrel, and T. Eisner. 1972. Struktur und Funktion des Drüsenepithels der postabdominalen Tergite von *Blatta orientalis. Z. Zellforsch. Mikrosk. Anat.* 125:45–87.
38. Pollard, H. B., C. J. Pazoles, C. E. Creutz, and O. Zinder. 1979. The chromaffin granule and possible mechanisms of exocytosis. *Int. Rev. Cytol.* 58:159–197.
39. Reggio, H. A., and G. E. Palade. 1978. Sulfated compounds in the zymogen granules of the guinea pig pancreas. *J. Cell Biol.* 77:288–314.
40. Simson, J. A. V., R. M. Dom, P. L. Sannes, and S. S. Spicer. 1978. Morphology and cytochemistry of acinar secretory granules in normal and isoproterenol-treated rat submandibular glands. *J. Microsc. (Oxf.).* 113:185–203.
41. Smith, N. K. R. 1979. A review of sources of spurious silicon peaks in electron microprobe x-ray spectra of biological specimens. *Anal. Biochem.* 94:100–104.
42. Steers, E., J. Beisson, and V. T. Marchesi. 1969. A structural protein extracted from the trichocyst of *Paramecium aurelia. Exp. Cell Res.* 57:392–396.
43. Tashiro, T., and H. Stadler. 1978. Chemical composition of cholinergic synaptic vesicles from *Torpedo marmorata* based on improved purification. *Eur. J. Biochem.* 90:479–487.
44. Taussky, H. H., and E. Shorr. 1953. A microcolorimetric method for the determination of inorganic phosphorus. *J. Biol. Chem.* 202:675–685.
45. Valverde, I., A. Vandermeers, R. Anjaneyulu, and W. J. Malaisse. 1979. Calmodulin activation of adenylate cyclase in pancreatic islets. *Science (Wash. D. C.).* 206:225–227.
46. VanLennep, E. W., A. R. Kennerson, C. G. Duck-Chong, and J. K. Pollak. 1978. Fine structure of the secretion granules in the mandibular gland of the echidna, *Tachyglossus aculeatus (Monotremata). Cytobiologie.* 18:1–9.
47. Wagner, J. A., S. S. Carlson, and R. B. Kelly. 1978. Chemical and physical characterization of cholinergic synaptic vesicles. *Biochemistry.* 17:1199–1206.
48. Winkler, H. 1976. The composition of adrenal chromaffin granules: an assessment of controversial results. *Neuroscience.* 1:65–80.